Structural Properties of the Putative Fusion Peptide of Fertilin, a Protein Active in Sperm−Egg Fusion, upon Interaction with the Lipid Bilayer †

ARTICLE *in* BIOCHEMISTRY · JANUARY 1999

Impact Factor: 3.02 · DOI: 10.1021/bi980909i · Source: PubMed

3 AUTHORS, INCLUDING:

Richard Epand
McMaster University
556 PUBLICATIONS **18,103** CITATIONS
SEE PROFILE

Jean-Marie Ruysschaert
Université Libre de Bruxelles
472 PUBLICATIONS **13,955** CITATIONS
SEE PROFILE

Structural Properties of the Putative Fusion Peptide of Fertilin, a Protein Active in Sperm−Egg Fusion, upon Interaction with the Lipid Bilayer[†]

Isabelle Martin,*[,‡] Richard M. Epand,[§] and Jean-Marie Ruysschaert[‡]

Laboratoire de Chimie-Physique des Macromolécules aux Interfaces (LCPMI), CP206/2, Université Libre de Bruxelles, 1050 Brussels, Belgium, and Department of Biochemistry, McMaster University, Health Sciences Center, 1200 Main Street West, Hamilton, Ontario, Canada L8N 3Z5

Received April 21, 1998; Revised Manuscript Received August 5, 1998

ABSTRACT: We recently demonstrated that a peptide representing the putative fusion domain of fertilin, a surface membrane protein of sperm involved in sperm−egg fusion, induces fusion of large unilamellar vesicles containing negatively charged lipids [Martin, I., and Ruysschaert, J. M. (1997) *FEBS Lett. 405*, 351−355]. In the present work, we demonstrate that increasing the concentration in negatively charged lipids strongly enhances the binding of the fertilin fusion peptide to the membrane, suggesting that electrostatic attractions play a crucial role in the binding process. While no significant change of the secondary structure content is observed by increasing the amounts of negatively charged lipids in the bilayer, the orientation of the α-helix changes from a parallel to an oblique orientation in the membrane. This topological change is confirmed by amide II hydrogen/deuterium exchange measurements that monitor the accessibility of the peptide to the water medium. Differential scanning calorimetry data also suggest that the fertilin fusion peptide lowers the bilayer to hexagonal phase transition temperature of model membranes composed of mixtures of dipalmitoleoylphosphatidylethanolamine and 1-palmitoyl-2-oleoylphosphatidylserine and therefore promotes negative curvature in lipid vesicles. A comparison of the biophysical properties and the membrane-perturbing activities of fertilin and of viral fusion peptides is discussed in terms of sperm−egg fusion and virus cell fusion.

Fertilin is a guinea pig sperm surface membrane protein which seems to play a role in sperm−egg membrane fusion (*1*, *2*). The two subunits, α and *β*, of fertilin share membrane topologies and other characteristics with viral binding and fusion proteins (*3*). The *β*-subunit contains a potential receptor binding domain, and the α-subunit contains a putative fusion peptide (*4*, *5*), suggesting that fusion events which occur during fertilization may share a common mechanism with penetration of enveloped viruses into host cells. Several lines of evidence supported a role of the *β*-subunit in particular, through its predicted integrin binding domain, in sperm adhesion to the egg plasma membrane (*6*−*8*). Indeed, peptide analogues of the predicted binding loops of the fertilin *β* disintegrin domain inhibit sperm−egg binding and fusion (*6*, *9*). The sequence recently suggested to be involved in fusion comprises residues 89−111 (His-Pro-Ile-Gln-Ile-Ala-Ala-Phe-Leu-Ala-Arg-Ile-Pro-Pro-Ile-Ser-Ser-Ile-Gly-Thr-Cys-Ile-Leu-Lys) of the α-subunit of fertilin (*4*). This sequence fulfills all three criteria of an internal fusion peptide: (a) located in a membrane-anchored subunit, (b) relatively hydrophobic, and (c) able to be modeled as a "sided" α-helix with most of the bulky hydrophobic residues on one face and charged amino acids on the other face (*5*). This peptide has been shown recently to interact with liposomes and to induce lipid mixing of large unilamellar vesicles (*10*, *11*).

Much of what is known regarding the molecular mechanism of viral membrane fusion has been gained using liposomes as model systems. Studies using model membranes, such as liposomes and synthetic peptides corresponding to the fusion regions of enveloped virus proteins, have revealed that the secondary structure and the orientation of the peptides when inserted into a lipid bilayer determine their fusogenic and lytic activities (*12*−*15*). These studies suggest that the unique oblique orientation of the viral fusion peptides modifies the average orientation of phospholipid acyl chains, facilitating the formation of inverted lipid phases as well as intermediates in membrane fusion. These intermediates have altered membrane curvature and allow for lipid mixing between bilayers (*13*, *16*−*18*). The good correlation already observed between the in vitro and in vivo experiments on SIV[1] (*14*, *19*) and HIV (*13*, *20*) proves the biological relevance of using model systems for examining the mech-

[†] This work was performed with the financial support of FNRS (Fonds National de la Recherche Scientifique), ARC (Action de Recherches Concertées), and the Medical Research Council of Canada (Grant MT-7654).

* Correspondence should be addressed to this author at Université Libre de Bruxelles, Campus Plaine CP 206/2, B-1050 Bruxelles, Belgium. Telephone: 32-02-650.53.66. FAX: 32-02-650.51.13. Email: imartin@ulb.ac.be.

[‡] Université Libre de Bruxelles.

[§] McMaster University.

[1] Abbreviations: PC, phosphatidylcholine; PS, phosphatidylserine; POPS, oleoylphosphatidylserine; PI, phosphatidylinositol; DPoPE, L-α-dipalmitoleoylphosphatidylethanolamine; DSC, differential scanning calorimetry; ATR-FTIR, attenuated total reflection Fourier transform infrared spectroscopy; T_H, transition temperature of bilayer to hexagonal phase; SIV, Simian immunodeficiency virus; LUV, large unilamellar vesicles; DMSO, dimethyl sulfoxide.

10.1021/bi980909i CCC: $15.00
Published on Web 11/10/1998

anisms by which an extramembranous segment of a transmembrane protein induces lipid bilayer fusion or membrane destabilization.

The molecular description of the lipid/fertilin peptide interaction should contribute to a better understanding of the molecular events involved in sperm−egg fusion and should reveal if fertilization and viral infection share a common fusion mechanism. In a previous study, we investigated the ability of the synthetic peptide corresponding to the putative fusion peptide of fertilin to destabilize and to induce lipid mixing of large unilamellar vesicles made of lipids mimicking the plasma membrane. Lipid mixing was shown to be dependent upon the presence of negatively charged lipids in the membrane (*11*). To get deeper insight into the molecular mechanism of membrane fusion induced by the fertilin peptide, we determined here how negatively charged lipids influence the secondary structure and the orientation of this peptide using Fourier transform infrared spectroscopy. This technique offers an excellent opportunity to study the structure of peptides in a lipid environment (*13*, *21*−*23*). Moreover, attenuated total reflection (ATR) infrared spectroscopy gives quantitative information about the orientation of the protein or peptide in a lipid matrix (*24*). Our data provide evidence that while no significant change of secondary structure is observed with an increasing amount of negatively charged lipid in the bilayer, the orientation of the helical fertilin peptide changes from a parallel to an oblique orientation in the membrane. Our data demonstrate that the binding of the fertilin fusion peptide to the lipid bilayer requires electrostatic interactions while viral fusion peptide binds largely through hydrophobic interactions. Interestingly, the two peptides insert obliquely into the lipid bilayer to promote fusion, suggesting that similar mechanisms may be involved in cell−cell and viral fusion.

MATERIALS AND METHODS

Materials. Egg phosphatidylcholine (PC) and bovine brain phosphatidylserine (PS) were purchased from Sigma Chemical Co. (St. Louis, MO). DPoPE and POPS were purchased from Avanti Polar Lipids (Alabaster, AL) and were used without further purification.

Calcein (Sigma) was purified by chromatography on Sephadex LH-20 (Pharmacia). Calcein was loaded on the column as a sodium salt solution and eluted with water at neutral pH. The concentration of calcein was determined spectrophotometrically, using 7.0×10^4 M^{-1} cm^{-1} as the molar extinction coefficient at 492 nm (*25*).

HPLC-purified synthetic peptide in its amide form was purchased from Chiron Mimotope. The peptides were dissolved in DMSO at a concentration of 1 mg/mL and stored at 4 °C.

Vesicles Preparation. Routinely, lipids were dissolved in chloroform at the desired concentrations, and the solution was dried under a stream of nitrogen to deposit a thin lipid film on the inside of a glass test tube. The film was further subjected to vacuum evaporation for 2−3 h to remove any trace of the solvent. Large unilamellar vesicles (LUV) were prepared by hydrating the dried lipid film with the Hepes buffer (10 mM Hepes, 150 mM NaCl, 0.1 mM EDTA, 0.02% NaN_3, pH 7.2), then repeatedly freezing and thawing the suspension 5 times, and finally extruding it 10 times through two polycarbonate filters of pore size 0.1 μm (Nucleopore Corp., Pleasanton, CA) using an extruder (Lipex Biomembranes Inc., Vancouver, Canada) according to the extrusion procedure of Mayer et al. (*26*). The prepared liposomes were stored at 4 °C until use.

Attenuated Total Reflection Fourier Transform Infrared Spectroscopy (ATR-FTIR). Spectra were recorded at room temperature on a Perkin-Elmer 1720X FTIR spectrophotometer equipped with a liquid nitrogen-cooled mercury cadmium telluride (MCT) detector at a nominal resolution of 4 cm^{-1}, and encoded every 1 cm^{-1}. The spectrophotometer was continuously purged with air, which had been dried on a silica gel column (5 × 130 cm). The internal reflection element was a germanium plate (50 × 50 × 2 mm, Harrick EJ2121) with an aperture angle of 45°, yielding 25 internal reflections. For each spectrum, 128 scan cycles were averaged; in each cycle, the sample spectra were ratioed against the background spectra of a clean germanium plate, using a shuttle to move the sample or reference into the beam. For polarization experiments, a Perkin-Elmer gold wire grid polarizer was positioned before the sample and the reference.

Samples Preparation. Samples were prepared by adding peptide, dissolved in DMSO at a final concentration of 1 mg/mL, to liposomes at various molar lipid/peptide ratios. After 1 h incubation at 37 °C, the lipid−peptide complex was separated from the free peptide on a Sephadex G-50 column (Pharmacia). Oriented multilayers were obtained by slow evaporation under a N_2 stream at room temperature (*24*) on one side of the germanium plate. To differentiate between the α-helix and the random structures, the multilayers were exposed for 3 h to D_2O-saturated N_2 (*27*).

Secondary Structure Determination. The determination of the secondary structure was based on the vibrational bands of protein or peptide, and particularly the amide I band (1600−1700 cm^{-1}), which is sensitive to the secondary structure (*28*). This amide I band, located in a region of the spectrum often free of other bands, is composed of 80% pure C═O vibration (*29*). The analysis was performed on the amide I region of deuterated samples because hydrogen/deuterium exchange allows differentiation of accessible α helix and irregular structures, the absorption band of which shifts from ∼1655 to 1642 cm^{-1} (*24*, *30*). Fourier self-deconvolution was carried out using a Lorentzian line shape for the deconvolution and a Gaussian line shape for the apodization. To quantify the area of the different components of amide I revealed by self-deconvolution, a least squares iterative curve fitting was performed to fit Lorentzian line shapes to the spectrum between 1700 and 1600 cm^{-1}. To avoid introducing artifacts due to the self-deconvolution procedure, the fitting was performed on the non-deconvoluted spectrum. Each band was assigned to a secondary structure according to the frequency of its maximum. The areas of all bands assigned to a given secondary structure were then summed up and divided by the total area. This ratio gives the proportion of the polypeptide chain in that conformation (*24*). The frequency limits for each structure were first assigned according to the data determined theoretically (*31*) or experimentally (*32*): 1662−1645 cm^{-1}, α-helix; 1689−1682 and 1637−1613 cm^{-1}, β-sheet; 1644.5−1637 cm^{-1}, random; 1682−1662.5 cm^{-1}, β-turns. These limits have been slightly adjusted to obtain a good agreement between the proportion of each structure determined by ATR-FTIR

and X-ray crystallography (*24*). This procedure extended to a series of well-characterized proteins provided a correct estimation of the α-helix and β-sheet structure content with a standard deviation of 8.7% when X-ray structures were taken as reference (*33*).

Orientation of the Secondary Structure. ATR-FTIR allows spectra to be recorded on ordered lipid bilayers and information to be gained about the orientation of different structures within proteins or peptides with respect to the bilayer (*24*, *34*). In an α-helix, the main transition dipole moment (C═O) is almost parallel to the helix axis while in an antiparallel β-sheet the polarization is opposite, predominantly perpendicular to the fiber axis (*29*). It is therefore possible to determine the mean orientation of the α-helix and β-sheet structures from the orientation of the peptide bonds corresponding to those of the C═O groups. Spectra were recorded with parallel (0°) and perpendicular (90°) polarized incident light with respect to the ATR plate. Polarization was expressed as the dichroic ratio $R_{atr} = A_{90}°/A_0°$. The mean angle between the C═O bond and a normal to the ATR plate surface is calculated from R_{atr} as described in Raussens et al. (*34*). The difference spectra are obtained by subtracting the 0° from the 90° polarization spectrum normalized to each other by zeroing the net integral of the intensities of the ester C═O stretching band of the *sn*-1 and *sn*-2 lipid chains in the 1710−1760 cm^{-1} region in the difference spectrum. The rationale behind this lies in the fact that both the *sn*-1 and the *sn*-2 carbonyl groups are found to make angles with respect to the bilayer normal that are close to the value for an isotropic orientation and their IR intensities are therefore expected to be independent of the polarization.

Kinetics of Deuteration. The oriented multilayers were obtained by slow evaporation of the liposomes under a N_2 stream, on a germanium plate as described above. Before starting the deuteration, 10 spectra were recorded to verify the reproducibility of the measurements and the stability of the system. At time 0, a D_2O-saturated N_2 flux was applied to the sample with a flow rate of 100 mL/min, controlled with a Brooks flow meter. The spectra at each time point were recorded on a Bruker IFS55 FTIR spectrophotometer and were the accumulation of 24 scans, with a resolution of 4 cm^{-1}. The signal from atmospheric water was subtracted as described by Goormaghtigh et al. (*24*). The amide I and II band areas were measured between 1700 and 1600 cm^{-1} and 1585−1502 cm^{-1}, respectively. The amide II area was divided by the amide I area for each spectrum to correct for any change in total intensity of the spectra during the deuteration process. This ratio, expressed between 0 and 100%, was plotted versus deuteration time. The 100% value is defined by the amide II/amide I ratio obtained before deuteration, whereas the 0% value corresponds to a zero absorption in the amide II region. It has been shown previously (*34*, *35*) on a series of proteins that can be fully denatured (and therefore fully deuterated) and then refolded to their native conformation, that complete H/D exchange results in 0 ± 5% absorption intensity in the amide II region. We are therefore confident that a zero absorbance in the amide II region corresponds to full deuteration of the protein.

Vesicle Leakage Assay. Dry lipid films were rehydrated to a concentration of 20 mg/mL in 10 mM HEPES buffer, pH 7.2, containing 62 mM calcein purified as described under Materials. Unencapsulated dye was removed by passing the liposome preparation over a Sephadex G-50 gel filtration column, equilibrated with 10 mM HEPES, 150 mM NaCl, 1 mM EDTA buffer, pH 7.2. Liposome concentration was estimated by measuring the lipid phosphorus content (*36*). Release of the fluorescent dye from preloaded LUV at a final lipid concentration of 3×10^{-4} M was monitored using an SLM 8000 spectrofluorimeter. Experiments were conducted in a 1 mL stirred cuvette, with right angle illumination. Excitation and emission wavelengths were set at 490 and 520 nm, respectively, employing slit widths of 4 nm. The addition of Triton X-100 to a final concentration of 0.1% (v/v) was used to determine maximal release. The percentage of total fluorescence was defined as

$$\% F_t = \frac{I_t - I_0}{I_{100} - I_0} \times 100$$

where I_0 is the initial fluorescence, I_{100} is the total fluorescence observed after addition of Triton X-100, and I_t is the fluorescence observed after addition of fusion peptide at t = 600 s, corrected for dilution.

Differential Scanning Calorimetry (DSC). DSC measurements were performed on a Microcal MC-2 high-sensitivity scanning calorimeter (Microcal Co., Amherst, MA). Lipid films were made from DPoPE dissolved in ice-cold chloroform to which varying quantities of peptide dissolved in ice-cold hexafluoropropanol were added. After solvent evaporation with nitrogen, final traces of solvent were removed in a vacuum chamber overnight. The lipid film was suspended in 20 mM PIPES, 1 mM EDTA, 150 mM NaCl with 0.002% NaN_3, pH 7.4, by vortexing at room temperature. The final lipid concentration was 15 mg/mL. The lipid suspensions were degassed 20 min under vacuum before being loaded into the calorimeter cell. A heating scan rate of 40 °C/h was employed. The bilayer to hexagonal phase transition was fitted to a single van't Hoff component and the transition temperature (T_H) reported as that for the fitted curve.

RESULTS

Secondary Structure Determination. The conformation of the fertilin fusion peptide in a membrane environment was determined by FTIR spectroscopy. This method is of particular value in studying membrane-bound peptides since the infrared measurements eliminate the potential artifacts due to light scattering of the vesicles. This method is based on the analysis of the vibration bands of protein or peptide, and particularly the amide I band ν(C═O), whose frequency of absorption is dependent upon the secondary structure (*24*).

When dissolved in DMSO, the fertilin peptide mainly adopts a β-sheet structure with a maximum absorbance at 1628 cm^{-1} (Table 1). This low frequency suggests that the β-strands are forming strong hydrogen bonds which may arise from intermolecular bonds between aggregated or oligomerized peptides (*37*). To study the effect of the lipid membrane on the secondary structure, the fertilin peptide was incubated with LUV of different compositions at pH 7.4 for 1 h at 37 °C. The membrane-bound peptide was separated from the free peptide by gel filtration on a G-50 column. When fertilin was incubated with LUV of egg PC, no association of the peptide to the lipid membrane was

Table 1: Proportion of Different Secondary Structures of Fertilin Fusion Peptide in the Absence and Presence of LUV of Different Compositions[a]

	FTIR secondary structure			
sample	α-helix (% ± 5%)	dichroic ratio	β-sheet (% ± 3%)	random (% ± 7%)
fertilin peptide in DMSO	20	−	60	20
PC/PS (80/20%)	46	0.92	30	25
PC/PI (80/20%)	45	n.d.	29	26
PC/PS (60/40%)	40	1.37	25	35

[a] The lipid to peptide molar ratio (100) before passage through a Sephadex G-50 column. The measurements were done after separation of vesicle-bound peptide from free peptide on a Sephadex G-50 column. nd = not determined.

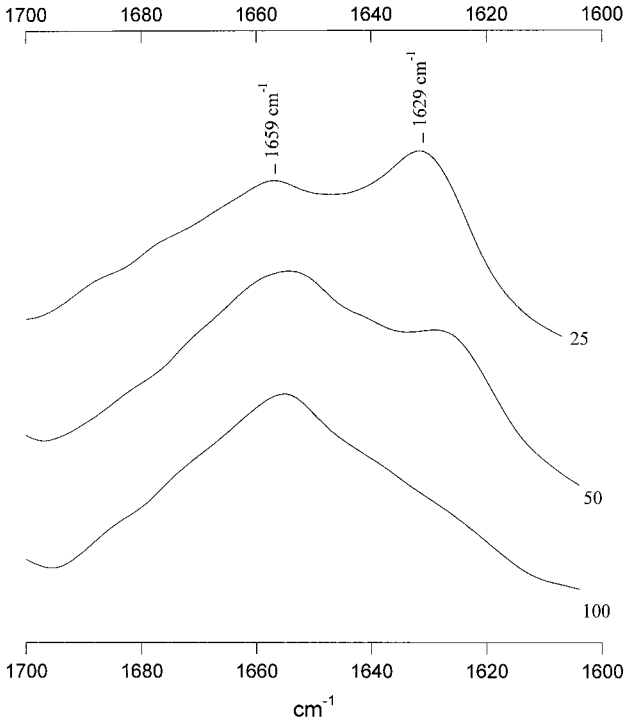

FIGURE 1: ATR-FTIR spectra between 1700 and 1600 cm^{-1} of the fertilin fusion peptide associated to LUV PC/PS (80/20%) at peptide to lipid molar ratios of 1/25, 1/50, and 1/100.

measured. Since it has been previously shown that negatively charged lipids such as PS or PI greatly increase the fusogenic and the lytic activity of the peptide (*11*), we incorporated various amounts of PS into the vesicle bilayer. Phosphatidylserine has been chosen because it is one of the most abundant phospholipids in the animal cell membrane. The FTIR-ATR spectra of fertilin associated to LUV of PC/PS (80/20%) were recorded in deuterated solvent at various lipid to peptide molar ratios (Figure 1). FTIR spectra of peptide bound to liposomes revealed a band centered around 1659 cm^{-1} characteristic of an α-helical conformation. There was a continuing shift to the α-helical conformation as the lipid to peptide ratio was increased (Figure 1), concomitant with a decrease of β-sheet content.

When the peptide was associated to LUV of PC/PS containing 40% negatively charged lipid instead of 20%, the FTIR spectra revealed the same shift to the α-helical region (Figure 2). A quantitative analysis of the amide I band of the deuterated spectra by Fourier self-deconvolution and least-squares curve fitting (*33*) allowed us to quantify the secondary structure of the peptide. For a lipid to peptide

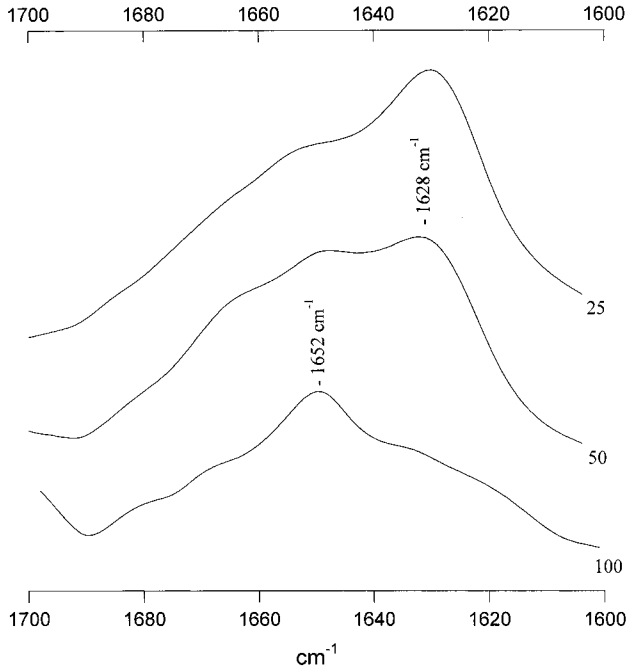

FIGURE 2: ATR-FTIR spectra between 1700 and 1600 cm^{-1} of the fertilin fusion peptide associated to LUV PC/PS (60/40%) at peptide to lipid molar ratios of 1/25, 1/50, and 1/100.

ratio of 100, evaluation of the secondary structure gives a content of α-helical and β-sheet structures of 46 ± 5% and 30 ± 5%, respectively, with 20% PS and 40 ± 5% and 25 ± 5% with 40% PS. All the spectra also displayed a component near 1640 cm^{-1} corresponding to a random structure, and contributing nearly 30% of the intensity of the amide I band (Table 1). The random component is probably associated with the COOH and NH_2 termini and is often observed for short peptides (*13*, *38*). To rule out a possible artifact due to lipid absorption, the spectra of vesicles containing 20% and 40% PS in the bilayer were recorded. Whatever the lipid composition, no absorption was detected between 1700 and 1600 cm^{-1} (data not shown).

The above structure determination demonstrates that the presence of negatively charged lipid is important for fertilin interaction with lipid bilayers but that the secondary structure is not sensitive to the amount of negatively charged lipids. It should be noted that the secondary structure is identical when PS is replaced by PI, suggesting that the fertilin peptide has no specificity for PS but only for a negatively charged lipid (Table 1).

Orientation of the Secondary Structure. Information about the orientation of a given secondary structure can be obtained by recording ATR-FTIR peptide spectra with polarized light, provided that the peptides are oriented with respect to the internal reflection element. This prerequisite is met with films formed from peptides inserted in lipid vesicles. Figure 3 displays the 90° − 0° difference polarization spectra of the fertilin peptide in PC/PS vesicles (80/20% or 60/40%). A coefficient was chosen to zero the lipid ν(C═O) band between 1700 and 1770 cm^{-1} as described previously (*27*). A positive deviation of the amide I band (between 1600 and 1700 cm^{-1}) in a polarization difference spectrum indicates an orientation of this dipole parallel to the lipid acyl chains, while a negative deviation corresponds to an orientation of the dipole perpendicular to the lipid acyl chains.

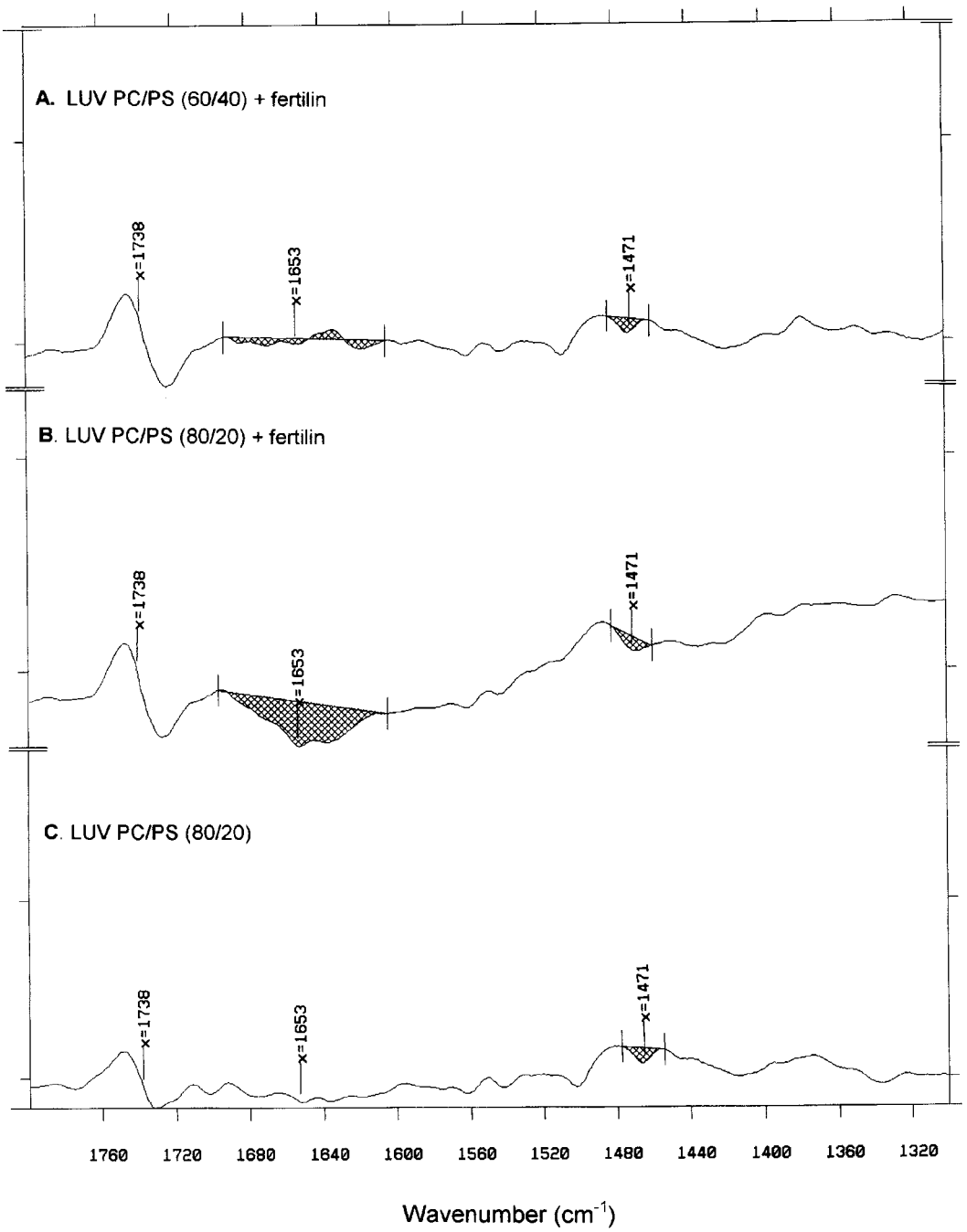

FIGURE 3: ATR dichroic spectra of fertilin associated to LUV at a lipid to peptide ratio of 100: (A) PC/PS (60/40 mol %), (B) PC/PS (80/20 mol %), and (C) PC/PS (80/20 mol %) without peptide. The dichroism spectra are obtained by subtracting the ATR spectra recorded with 0° polarization from the 90° recorded spectra. The difference spectra are normalized by zeroing the net integral of the intensity of the ester C═O stretching bands of the *sn*-1 and *sn*-2 chains in the 1710−1760 cm^{-1} region of the difference spectrum. The dichroic spectra are expanded 3-fold in the ordinate direction.

For the fertilin peptide associated to LUV of PC/PS (80/20%), a negative deviation was observed in the amide I (C═O) region of the difference spectrum (Figure 3B), whereas no deviation was observed when the peptide was inserted into LUV of PC/PS (60/40%) (Figure 3A). These patterns indicate that the orientation of the α-helical structure of fertilin changes with the amount of negatively charged lipid in the bilayer. When 20% PS is present in the membrane, the α-helix associated with the fertilin peptide essentially lies parallel to the membrane surface. An increase in the amount of PS modifies the orientation from parallel to an intermediate orientation, which is neither parallel nor perpendicular to the ATR element surface.

The dichroic ratio of the α-helical component was calculated from the following equation (*34*) assuming that the α-helices are the only strongly oriented components:

$$R_\alpha = \frac{R - [(R+2)/(2R_{iso}+1)](1-x)}{1 - (1/R_{iso})[(R+2)/(2R_{iso}+1)](1-x)}$$

where R_α is the dichroic ratio of the α-helical component, R is the measured dichroic ratio (area amide I 90°/area amide I 0°), $R_{iso} = 1.49$ is the ratio of the intensities at 90° and 0° of a dipole with an isotropic orientation (the C═O stretching band of the *sn*-1 and *sn*-2 lipid chains in the 1710−1760 cm^{-1} region), and x is the fraction of α-helical structure.

The angle between the long axis of the α-helix and a normal to the germanium plate is calculated from this dichroic ratio. Taking into account the α-helical content reported in Table 1, the calculated dichroic ratio of 0.92 ± 0.05 corresponds to an angle of 0 ± 5° between the α-helix and the germanium plate for the fertilin peptide associated to LUV of PC/PS (80/20%), while for the peptide associated to LUV of PC/PS (60/40%) the dichroic ratio of 1.37 ± 0.03 corresponds to an angle of 45 ± 5°. The relationship between the dichroic ratio and the orientation of a given structure (α-helix in this case) is dependent upon the angle between the transition dipole being considered and the primary axis of the structure (*24*). The above angle was calculated with an order parameter of 1 and a value of 27° for the angle between the C═O dipole and the helix axis (*24*).

Efforts have been made to characterize the orientation of the phospholipids in the bilayer in order to assess the overall membrane orientation on the germanium plate in the absence and the presence of peptide. In the absence of peptide, the phospholipid $\omega(CH_2)$ vibration near 1468 cm^{-1}, whose transition dipole moment is perpendicular to the axis of the lipid acyl chain, appears as a negative deviation on the dichroic ratio spectra (obtained by subtracting the 0° spectrum from the 90° spectrum). This demonstrates that the phospholipid acyl chains are oriented almost perpendicular to the germanium plate; i.e., the bilayer lies parallel to the germanium plate (Figure 3C). The dichroic ratio of the $\omega(CH_2)$ vibration at 1468 cm^{-1} is 1.00 ± 0.05 without or with peptide, and is consistent with a well-ordered lipid bilayer oriented parallel to the plane of the germanium plate. The fact that the peptide did not affect the lipid organization is probably due to the low peptide to lipid molar ratio (1/200). Tamm and Tatulian (*39*) have demonstrated that only at peptide to lipid molar ratios up to 1/20, small hydrophobic peptides are able to disturb the orientational order of the lipid molecules to a significant degree.

Amide Hydrogen/Deuterium Exchange Kinetics. To further characterize the conformational change taking place upon lipid binding, the kinetics of deuteration of the fertilin fusion peptide associated to LUV PC/PS (80/20%) and LUV PC/PS (60/40%) were measured. At constant pH (7.2) and temperature (20 °C), the rate of amide hydrogen/deuterium exchange is related to the stability of the secondary structure and to the solvent accessibility of the NH amide group of the protein or peptide. Amide hydrogen exchange was measured by monitoring the decrease in the amide II absorption (maximum at 1544 cm^{-1}) as a function of the time of exposure to D_2O-saturated N_2 (from 15 s to 2 h; for details, see Materials and Methods). The percentage of deuteration of fertilin peptide associated to LUV of PC/PS (80/20%) and PC/PS (60/40%) (Figure 4) was calculated from the amide II /amide I ratio as described under Materials and Methods. Hydrogen/deuterium exchange was faster and almost complete for the peptide associated to the LUV containing 20% negatively charged lipids. After 20 min deuteration, 90% of the peptide N−H groups were exchanged, suggesting a complete accessibility of the peptide to the solvent, while when the fertilin peptide was associated to vesicles containing 40% PS, only 20% of the peptide NH groups were exchanged, suggesting less accessibility of the peptide to the solvent. This result fully confirms the FTIR orientation; i.e., for vesicles containing 20% PS, the helix is parallel to the lipid membrane and accessible to the solvent, while for vesicle containing 40% PS the helix is inserted in the lipid bilayer and much less accessible to the solvent.

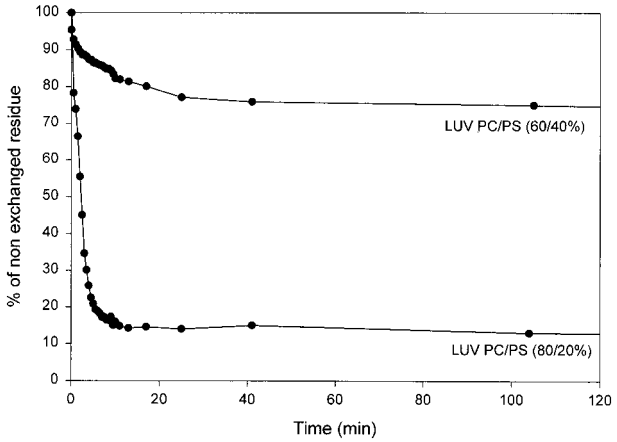

FIGURE 4: Evolution of the proportion of non-exchanged residues as a function of the deuteration time. The film of the samples spread on a germanium plate was exposed to a D_2O-saturated N_2 flux, and the spectra were recorded automatically with increasing time as described under Materials and Methods. The amide II/I area for each spectrum, which was expressed between 0% and 100%, was reported as a function of deuteration time.

Determination of an Apparent Binding Constant of Fertilin Peptide to PC/PS Vesicles. In earlier experiments, we observed that the fertilin peptide interacted only with liposomes having a negative charge. We also demonstrated that this peptide promoted membrane fusion as measured by lipid mixing as well as calcein release (*11*). In the present work, we have more systematically studied the role of negatively charged lipids on calcein release. The calcein release increases with an increased amount of PS in the lipid bilayer (Figure 5). Virtually, no calcein release was observed with the uncharged vesicles even at high fertilin peptide concentration (data not shown), suggesting that an electrostatic component is involved in the interaction of the fertilin fusion peptide with the lipid membrane.

To determine an apparent binding constant of the fertilin peptide to PC/PS vesicles containing various amounts of PS (5, 20, and 40%), calcein release was measured as a function of peptide concentration for three different lipid concentrations (66, 132, and 264 μM). The leakage rate depended on both the peptide and the lipid concentrations: an increase in the peptide concentration or a decrease in the lipid concentration resulted in an enhanced leakage rate as shown in Figure 6A for LUV of PC/PS (60/40%), suggesting that the leakage rate was determined only by the amount of membrane-bound peptide per lipid molecule (*r*) (*40*). This ratio, *r*, is determined by the total peptide concentration, [P], the free peptide concentration, P_f, and the lipid concentration, *L*, through the mass equation $[P] = P_f + rL$ (for a more detailed description, see *41*). Figure 6B shows that [P] is a linear function of *L* (between 10% and 50% release), in agreement with the above equation. According to the mass equation, the *r* and P_f values were obtained from the slopes and the intercepts, respectively. The relationship between *r* and P_f values is shown in Figure 7 for the different lipid vesicles composition. An apparent binding constant was calculated by linearly extrapolating the curve to zero concentration of free peptide (*40*, *42*). Values of K_{app} were 3×10^8, 0.9×10^7, and 1×10^6 M^{-1}, respectively, for 40%,

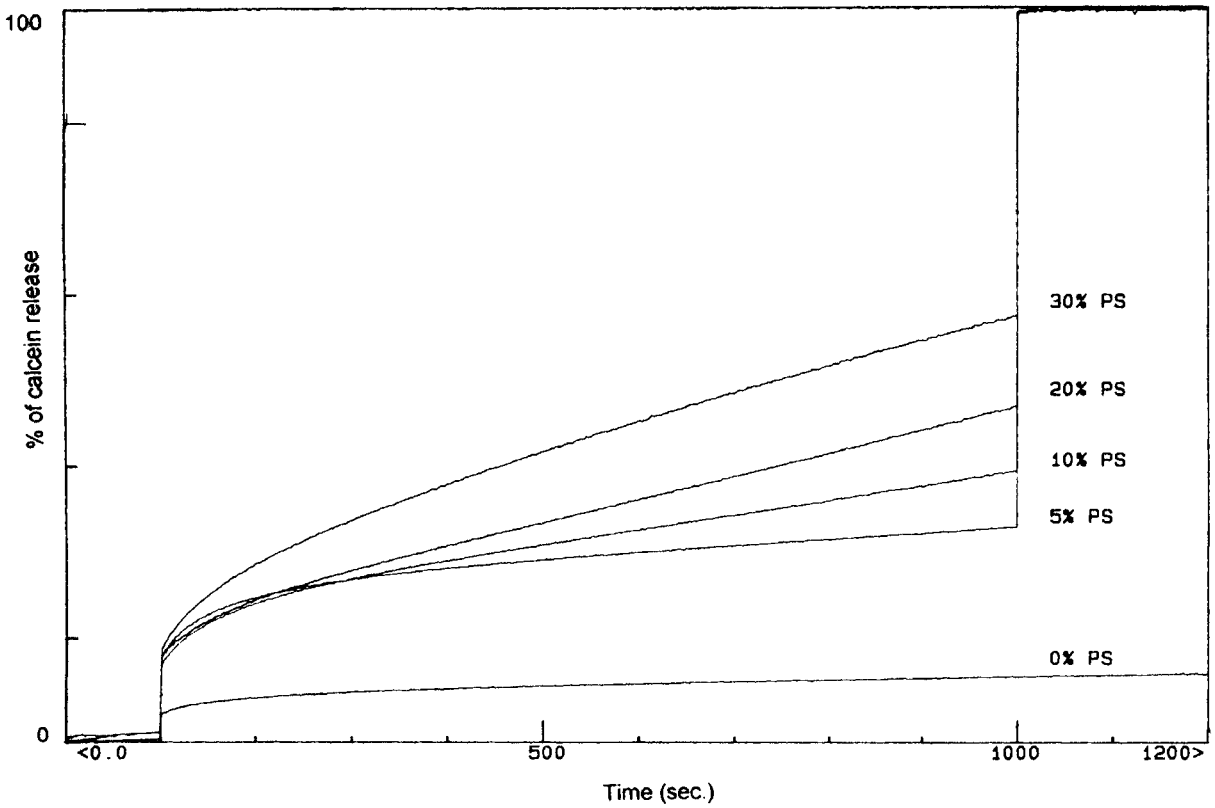

FIGURE 5: Effects of negatively charged lipids on the leakage of entrapped calcein out of PC/PS LUV: time course of calcein leakage with increasing amounts of PS in the lipid bilayer. The leakage of the dye was monitored at 37 °C. The peptide and the lipid concentrations were 3 nM and 132 μM, respectively. The peptide was added to the vesicles suspension at $t = 100$ s. Dimethyl sulfoxide (DMSO) up to 2% (v/v), which is the maximal concentration used, did not modify the fluorescence.

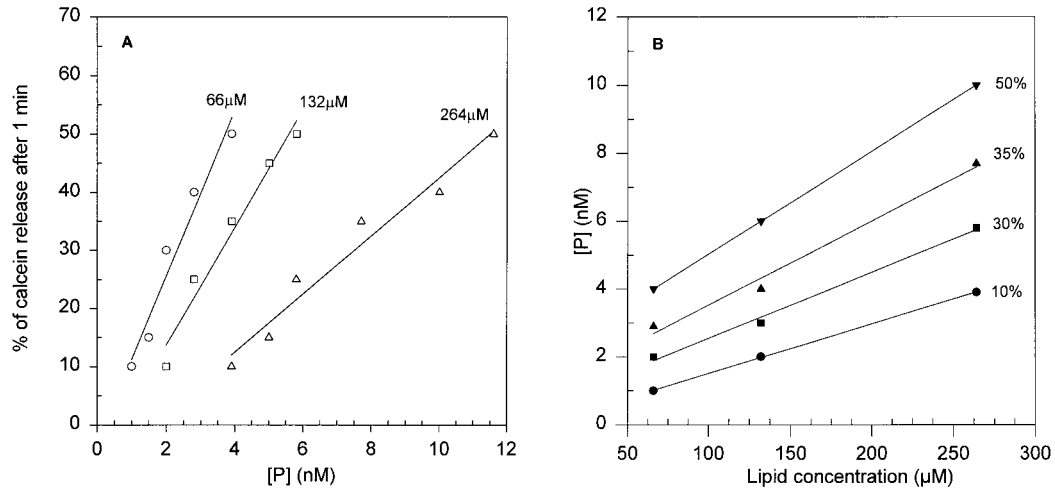

FIGURE 6: (A) Effect of fertilin peptide and lipid concentrations on the release of calcein. Percentages of calcein released from LUV of PC/PS (60/40%) were determined at various concentrations of fertilin and of lipid at 1 min after addition of the peptide. (B) Estimation of free and membrane-bound peptide concentration. Different pairs of P and L values, for which a given leakage (between 15% and 50%) was measured, were plotted according to the equation in the text. The free peptide concentration and the number of membrane-bound peptides per lipid molecule, r, were evaluated from the intercept and the slope, respectively. The lipid composition used in these experiments was PC/PS (60/40%).

20%, or 5% PS in the lipid bilayer. This demonstrates that fertilin has a higher affinity for lipid membranes with a higher content of negatively charged lipids and that negatively charged acidic phospholipids are necessary for effective binding. It should be noted that these apparent binding constants were obtained by measuring the efficiency of the fertilin fusion peptide in destabilizing the lipid membrane. Therefore, the 10−100 times difference observed among the membranes with different percentages of PS could result from two different mechanisms, i.e., an increase in the amount of peptide bound to the lipids or an increase in the efficiency of the bound peptide in destabilizing the membrane. We have no experimental evidence to discriminate between these hypotheses.

Effect of the Fertilin Peptide on T_H of DPoPE. To better characterize the effect of fertilin on the lipid bilayer organization, we have measured by DSC the effect of the fusion peptide on the transition temperature of bilayer to

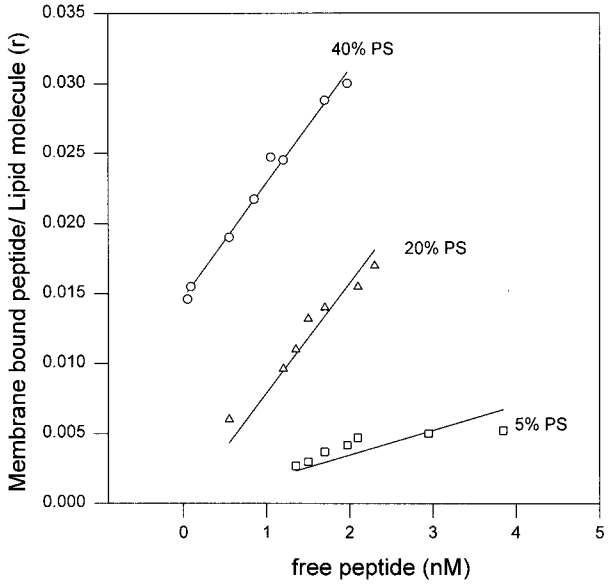

FIGURE 7: Evaluation of the apparent binding constant of fertilin to LUV of PC/PS. Binding isotherms of fertilin fusion peptide calculated as described in the text for 5, 20, and 40% PS. For LUV of PC/PS (60/40%), r and P_f were evaluated from the slope and the intercept of the curves in Figure 6B.

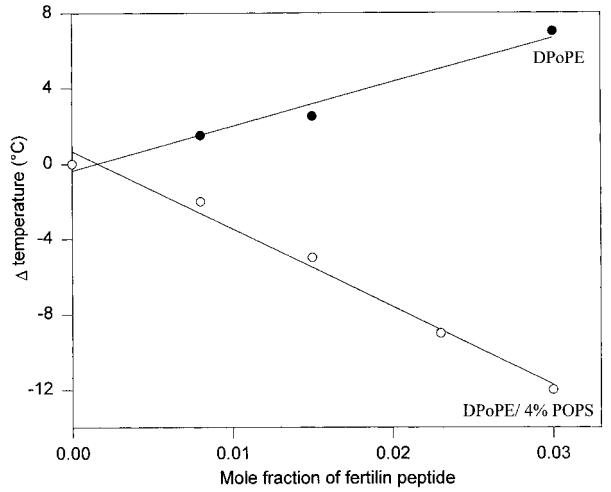

FIGURE 8: Shift in T_H of DPoPE in the absence or in the presence of POPS and as a function of mole fraction of peptide. Temperatures from DSC heating scans at 40 °C/h in buffer at pH 7.4.

hexagonal phase (T_H). Incorporation of different amounts of the fertilin peptide in DPoPE multilamellar vesicles increases T_H (Figure 8). We also evaluated the T_H of liposomes containing various amounts of POPS. In the presence of 2 and 4 mol % POPS, the T_H was raised by 3 and 5 °C, respectively (data not shown). Addition of fertilin to DPoPE/2% POPS induces a shift to higher T_H as has been observed for pure DPoPE. However, when the membrane contained 4% POPS, T_H was shifted in the opposite direction, i.e., to lower temperature by the fertilin peptide (Figure 8). The extent of the shift with the fertilin peptide, -416 ± 100 °C/mole fraction peptide, is similar to the value, -453 ± 112 °C/mole fraction peptide, which was previously found for the influenza fusion peptide at acidic pH (*43*) or -360 ± 100 °C/mole fraction peptide found for the SIVwt fusion peptide (*44*). Thus, the fertilin fusion peptide in the presence of 4% POPS in the lipid bilayer has the same ability to destabilize a membrane bilayer as do viral fusion peptides.

DISCUSSION

A general conclusion from studies on biological membrane fusion is that this process is mediated by proteins (*5*, *45*, *46*), although little is known about the mechanism by which these proteins mediate membrane fusion. Recently, a protein from guinea pig sperm, fertilin, was purified using an antibody that blocks sperm−egg fusion (*1*, *2*). The cloning and sequencing of this protein revealed a putative fusion peptide in the α-subunit. In a previous paper, we demonstrated that a synthetic peptide corresponding to this putative fusion peptide of fertilin induced lipid mixing of large unilamellar vesicles and release of an encapsulated fluorescence dye from the lipid vesicles (*11*). Both processes required the presence of negatively charged lipids in the membrane. It should be noted that the determining parameter is not the nature of the acidic lipid but rather the presence of negatively charged lipids at the membrane surface. Substitution of PS by PI in the vesicles used for the different experiments described in this study did not modify the lipid destabilization.

The ATR-FTIR study supports a model where the peptide, upon binding to the lipid phase, adopts an almost helical conformation with unordered structures only at the ends of the helix. The contribution of the β-structure was weak, suggesting that the β-sheet is not the main structure of membrane-bound fertilin peptide. Earlier studies on this peptide by CD and FTIR measurements concluded that the preferred conformation of the peptide in a lipid environment is a β-sheet structure (*10*, *47*). However, in these experiments the unbound peptide was not separated from the inserted peptide, and the observed β-sheet structure could be due to aggregated peptide.

Since the helicity of the fertilin peptide is comparable in the presence of 20% or 40% negatively charged lipid in the bilayer, for the different lipid to peptide ratios another parameter must be involved to explain the increased lytic activity of the peptide at higher PS concentrations. An important physical parameter, which could potentially discriminate between functional and nonfunctional fusion peptides, is the orientation in the membrane of the α-helices. Polarized ATR-FTIR spectroscopy has been demonstrated to be a powerful tool in determining the orientation of protein and peptides into a lipid bilayer (*24*, *28*). Orientation of α-helical peptides in a lipid membrane has been successfully assigned in several instances by this method, for example, melittin (*48*), pulmonary surfactant proteins (*22*), GALA peptide (*49*), or a synthetic signal peptide (*21*). Applying this method to the fertilin peptide in the presence of various amounts of negatively charged lipids revealed that an increase from 20% to 40% PS significantly changes the orientation of the α-helix relative to the lipid bilayer, increasing the angle to 45° with respect to the plane of the membrane. It should be pointed out that FTIR spectroscopy does not discriminate between a fixed uniaxial orientation and the motional averaging of different orientations. The parallel orientation observed for the peptide in the presence of 20% PS in the lipid bilayer cannot rule out the existence of a minor peptide population adopting an oblique orientation and destabilizing the membrane. The hydrogen/deuterium exchange data fully agreed with the change in the orientation of the α-helix when the amount of PS in the lipid bilayer was increased. In the presence of 20% PS, the peptide is highly accessible to the

solvent, and the α-helix is oriented parallel to the membrane, while in the presence of 40% PS, the low H/D exchange supports the view that the α-helix is more deeply inserted into the lipid bilayer.

The oblique orientation of the fertilin peptide described above has already been described for viral fusion peptides such as SIV (*14*, *19*), HIV (*13*), and Influenza (*38*). A possible mechanism by which these peptides, when obliquely inserted into lipid membranes, may perturb bilayer packing is by expanding the center of the bilayer more than the bilayer surface. Such a situation would increase the negative curvature strain and favor the formation of inverted phases. There is some evidence that viral fusion peptides may promote fusion by destabilizing bilayers in this way (*43*, *44*). Our DSC data indicate that the incorporation of the fertilin fusion peptide into DPoPE/POPS bilayers decreases the transition temperature of the bilayer to the hexagonal phase. Such an effect on this phase transition has already been observed with DPoPE for viral fusion peptides such as SIV (*44*) and Influenza (*43*). DSC experiments described in this study and in the literature show that three fusion peptides with different motifs (the SIV being all hydrophobic, the Influenza having acidic amino acid residues, and fertilin having basic amino acid residues), involved in different fusion processes, promoted inverted phase formation in model membranes when they are in a fusion-active form. The DSC experiment was not carried out using conditions corresponding to the FTIR and vesicle leakage studies since we were not attempting to demonstrate a correlation between H_{II} phase formation and vesicle fusion. We used the shifts in T_H to test if the peptide favored or disfavored the formation of an inverted phase (i.e., if it lowered or raised T_H). Anionic lipid was added to POPE to facilitate the binding of the peptide to the lipid. Higher mole fractions of anionic lipid would have resulted in broad phase transitions, and it would not have been possible to determine the effects of the peptide on T_H in such mixtures. The finding is most relevant in terms of the direction of the change in T_H and not of the absolute extent of this change. The results also demonstrate that the presence of anionic lipid is required for the peptide to lower T_H.

As a conclusion, some strong similarities and key differences can be discerned in the behavior of the fertilin and viral fusion peptides (*50* and references cited within). A first difference is that electrostatic interaction between the positive charge of the fertilin peptide and the negative charge of the membrane surface plays a crucial role in peptide binding and insertion into the membrane. In comparison, viral fusion peptide binding is essentially hydrophobic. The binding of the fusion peptides induced the same conformational change in the two cases, illustrating the role of an α-helical structure to maintain the fusion activity of the peptide. One major similarity between the two types of peptides is that the two kinds of fusion peptide insert with an oblique orientation into the lipid membrane. The insertion of the peptide would expand the center of the bilayer, more than the bilayer surface, and would thereby increase the negative curvature strain of the host cell.

REFERENCES

1. Primakoff, P., Hyatt, D. G., and Tredick-Kline, J. (1987) *J. Cell Biol. 104*, 140−149.
2. Blobel, C. P., Myles, D. G., Primakoff, P., and White, J. (1990) *J. Cell Biol.*, 67−78.
3. Wolfsberg, T., Bazan, F., Blobel, C., Myles, D., Primakoff, P., and White, J. (1993) *Proc. Natl. Acad. Sci. U.S.A. 90*, 10783−10787.
4. Blobel, C. P., Wolfsberg, T. G., Turck, C., Myles, D. G., Primakoff, P., and White, J. M. (1992) *Nature 356*, 248−252.
5. White, J. M. (1992) *Science 258*, 917−924.
6. Myles, D. G., Kimmel, L. H., Blobel, C. P., White, J. M., and Primakoff, P. (1994) *Proc. Natl. Acad. Sci. U.S.A. 91*, 4195−4198.
7. Almeida, E. A. C., Huovila, A.-P. J., Sutherland, A. E., Stephens, L. E., and Calarco, P. G. (1995) *Cell 81*, 1095−1104.
8. Evans, J. P., Schultz, R. M., and Kopf, G. S. (1995) *J. Cell Sci. 108*, 3267−3278.
9. Snell, W., and White, J. M. (1996) *Cell 85*, 629−637.
10. Muga, A., Neigebauer, W., Hirama, T., and Surewicz, W. K. (1994) *Biochemistry 33*, 4444−4448.
11. Martin, I., and Ruysschaert, J.-M. (1997) *FEBS Lett. 405*, 351−355.
12. Lear, J. D., and Degrado, W. (1987) *J. Biol. Chem. 262*, 6500−6505.
13. Martin, I., Schaal, H., Scheid, A., and Ruysschaert, J. M. (1996) *J. Virol. 70*, 298−304.
14. Martin, I., Dubois, M. C., Defrise-Quertain, F., Saermark, T., Burny, A., Brasseur, R., and Ruysschaert, J. M. (1994) *J. Virol. 68*, 1139−1148.
15. Nieva, J. L., Nir, S., Muga, A., Goni, F., and Wilschut, J. (1994) *Biochemistry 33*, 3201−3209.
16. Colotto, A., Martin, I., Ruysschaert, J. M., Sen, A., Hui, S. W., and Epand, R. M. (1996) *Biochemistry 35*, 980−990.
17. Colotto, A., and Epand, R. M. (1997) *Biochemistry 36*, 7644−7651.
18. Siegel, D., and Epand, R. M. (1997) *Biophys. J. 73*, 3089−3111.
19. Horth, M., Lambrechts, B., Marinee, C., Bex, F., Thiriart, C., Ruysschaert, J.-M., Burny, A., and Brasseur, R. (1991) *EMBO J. 10*, 2747−2755.
20. Schaal, H., Klein, M., Gehrmann, P., Adams, O., and Scheid, A. (1995) *J. Virol. 69*, 3308−3314.
21. Goormaghtigh, E., Martin, I., Vandenbranden, M., Brasseur, R., and Ruysschaert, J. M. (1989) *Biochem. Biophys. Res. Commun. 158*, 610−616.
22. Vandenbussche, G., Clercx, A., Clercx, M., Curstedt, J., Johansson, J., Jörnvall, H., and Ruysschaert, J. M. (1992) *Biochemistry 31*, 9169−9176.
23. Clercx, A., Vandenbussche, G., Curstedt, T., Johansson, J., Jörnvall, H., and Ruysschaert, J. M. (1995) *Eur. J. Biochem. 229*, 465−472.
24. Goormaghtigh, E., Cabiaux, V., and Ruysschaert, J. M. (1994) *Subcell. Biochem. 23*, 329−450.
25. Allen, T. M., and Cleland, L. G. (1980) *Biochim. Biophys. Acta 597*, 418−426.
26. Mayer, L. D., Hope, M. J., and Cullis, P. R. (1986) *Biochim. Biophys. Acta 858*, 161−168.
27. Cabiaux, V., Brasseur, R., Wattiez, R., Falmagne, P., Ruysschaert, J.-M., and Goormaghtigh, E. (1989) *J. Biol. Chem. 264*, 4928−4938.
28. Fringeli, U. P., and Günthard, H. H. (1981) *Mol. Biol. Biochem. Biophys. 31*, 270−332.
29. Gremlich, H. U., Fringeli, U. P., and Schwyzer, R. (1983) *Biochemistry 22*, 4257−4264.
30. Cortijo, M., Alonso, A., Gomez-Fernandez, J. C., and Chapman, D. (1982) *J. Mol. Biol. 157*, 597−618.
31. Krimm, S., and Bandekar, J. (1986) *Adv. Protein Chem. 38*, 181−364.
32. Byler, D. M., and Susi, H. (1986) *Biopolymers 25*, 459−487.
33. Goormaghtigh, E., Cabiaux, V., and Ruysschaert, J.-M. (1990) *Eur. J. Biochem. 193*, 409−420.
34. Raussens, V., Ruysschaert, J. M., and Goormaghtigh, E. (1997) *J. Biol. Chem. 272*, 262−270.
35. de Jongh, H. H., Goormaghtigh, E., and Ruysschaert, J. M. (1996) *Anal. Biochem. 242*, 95−103.
36. Msrny, R. J., Volwerk, J. J., and Griffith, O. H. (1986) *Chem. Phys. Lipids 39*, 185−191.

37. Jackson, M., and Mantsch, H. M. (1995) *CRC Crit. Rev. Biochem. Mol. Biol. 30*, 95−120.
38. Lüneberg, J., Martin, I., Nussler, F., Ruysschaert, J. M., and Herrmann, A. (1995) *J. Biol. Chem. 270*, 27606−27614.
39. Tamm, L., and Tatulian, S. (1993) *Biochemistry 32*, 7720−7726.
40. Matsuzaki, K., Nakai, S., Handa, T., Takaishi, Y., Fujita, T., and Miyajima, K. (1989) *Biochemistry 28*, 9392−9398.
41. Matsuzaki, K., Harada, M., Funakashi, S., Fujii, N., and Miyajima, K. (1991) *Biochim. Biophys. Acta 1063*, 162−170.
42. De Geyter, C., Vogt, B., Benjelloun-Touimi, Z., Sansonetti, P., Ruysschaert, J. M., Parsot, C., and Cabiaux, V. (1997) *FEBS Lett. 400*, 149−154.
43. Epand, R. M., and Epand, R. F. (1994) *Biochem. Biophys. Res. Commun. 202*, 1420−1425.
44. Epand, R. F., Martin, I., Ruysschaert, J.-M., and Epand, R. M. (1994) *Biochem. Biophys. Res. Commun. 205*, 1938−1943.
45. Stegmann, T., White, J. M., and Helenius, A. (1990) *EMBO J. 9*, 4231−4241.
46. Kowalski, M., Potz, J., Basiripour, L., Dorfman, T., Goh, W., Terwilliger, E., Dayton, A., Rosen, C., Haseltine, W., and Sodroski, J. (1987) *Science 237*, 1351−1355.
47. Niidome, T., Kimura, M., Chiba, T., Ohmor, N., Hara, H., and Aoyagi, H. (1997) *J. Peptide Res. 49*, 563−569.
48. Weaver, A. J., Kemple, M. D., Brauner, J. W., Mendelshon, R., Pendergast, F. G. (1992) *Biochemistry 31*, 1301−1313.
49. Goormaghtigh, E., De Meutter, J., Szoka, F., Cabiaux, V. Parente, R., and Ruysschaert, J. M. (1990) *Eur. J. Biochem. 195*, 421−429.
50. Durell, S., Martin, I., Ruysschaert, J. M., Shai, Y., and Blumenthal, R. (1997) *Mol. Membr. Biol. 14*, 97−112.

BI980909I